

MODEL OF POROUS MATERIAL SINTERING

*O.V. Shults, V.A. Simonenko, S.P. Drovosekov, P.V. Kapustina,
I.A. Belobrova*

Russian Federal Nuclear Center, Snezhinsk, Russian Federation

E-mail: o.v.shults@vniitf.ru, v.a.simonenko@vniitf.ru, s.p.drovosekov@vniitf.ru,
p.v.kapustina@vniitf.ru, i.a.belobrova@vniitf.ru

The mathematical model of inert porous materials sintering was proposed. As an initial data, the model uses the initial distribution of pore surface elements and time-temperature conditions of sintering. Sintering is modelled by the system of kinetic equations describing shrinkage of a material depending on its initial properties and a time-temperature condition of the process. Experiments on aluminum oxide powder sintering have been carried out in several time-temperature conditions in which linear shrinkage was traced in time. The initial powder particles size distribution was previously measured. A value of main parameters used in the model was determined according to the sample linear shrinkage data measured at the 10 °C/min heating rate. Time dependences of linear shrinkage were calculated for the heating rates of 5 and 15 °C/min. Comparison of the calculated dependences with experimental data for heating rates 5 and 15 °C/min has shown the good qualitative and quantitative concordance.

Keywords: sintering; ceramics; mathematical modelling.

Introduction

Sintering process is an important and difficult stage of the ceramics manufacturing process. Main characteristics of a targeted ceramic product, i.e. its composition, structure, form, and sizes, are determined at the sintering stage [1]. So, estimation the optimal sintering mode and the appropriate input parameters of the initial material is very important for ceramic manufacturing optimization. Currently, mathematical simulation turns out to be a promising and efficient way of process optimization as it enables series of numerical experiments for targeted conditions thus reducing the number of physical experiments and also identification of main factors preconditioning the process result.

A good few approaches to sintering modelling are currently available. Many of them describe the process by applying a certain set of stages and the system state – using a simplified geometry of particles [2–5].

This paper proposes a sintering process model as applied to the alumina ceramics. Key points in this model are the following. The entire process is presented to be continuous and the system is described through the general-surface state that is characterized by the distribution of elements having certain curvature and volume.

1. Description of the Model

A phenomenological model is proposed to describe the powder sintering process. This model is based on a set of the following assumptions:

1. A porous body is characterized by a single surface with the area being equal to the total surface area of all particles;

2. The general surface of the porous body can be broken up into a great number of spherical elements with certain radii and volumes corresponding there too (in the strict sense, a pair of radii must correspond to each element in the case of a three-space surface but the given approach uses only one radius);

3. Any state of the porous body can be presented as a certain distribution of the above spherical elements depending on curvature radii:

$$dn_r = \phi(r) \cdot dr, \quad (1)$$

where n_r is the number of fraction elements of radius r , $\phi(r)$ is the density function;

4. The driving force of the mass-transfer is directed from the smaller-radius elements to the greater-radius elements as the greater capillary pressure p_c (Pa) corresponds to the less radius

$$p_c = \frac{\sigma}{2r}, \quad (2)$$

where σ is the surface tension (J/m²), r is the surface curvature radius (m);

5. Sintering kinetics depends on the vacancy flux between each combination of element fractions; the vacancy flux from the i -th fraction of elements into the j -th f_{ij} is proportional to the vacancy mobility k , the permeability of the porous body for the vacancy flux p , the driving force ΔH_{ij} (differences in curvature values for elements of the i -th and j -th fractions) and the product of volumetric concentrations of interacting elements C_i and C_j

$$f_{ij} = k \cdot p \cdot \Delta H_{ij} \cdot C_i \cdot C_j. \quad (3)$$

The vacancy mobility k is determined from the Arrhenius equation:

$$k = A \cdot \exp \left[-\frac{E}{RT} \right], \quad (4)$$

where A is the pre-exponential factor (m¹¹/s), E is the activation energy (J/mole), R is the gas constant (8,314 J · mole⁻¹ · K⁻¹), and T is the temperature (K).

The surface diffusion is considered to be the main transport mechanism and, correspondingly, the permeability of the porous body p for the vacancy flux is taken to be proportional to the specific surface of the body

$$p = \frac{S_g}{V_p + V_c}. \quad (5)$$

where S_g is the general surface of the porous body (m²), V_p is the total volume of pores (m³), V_c is the volume of the crystalline material (m³).

The spherical elements curvature H (m⁻¹) is determined from the formula

$$H = \frac{1}{r}, \quad (6)$$

where r is the sphere radius (m). The volumetric concentration of elements C is determined from the formula

$$C = \frac{n}{V_p + V_c}, \quad (7)$$

where n is the number of elements.

Then, the rate of changes in the number of elements of the i -th fraction will be

$$\frac{\partial n_i}{\partial t} = -\frac{\sum_j f_{ij}}{V_i}, \quad (8)$$

where t is the time (s), V_i is the volume of one element of the i -th fraction (m^3).

Pursuant to the assumption on the external-to-internal surface equivalency, the external surface is considered as the only element with the negative curvature (in the strict sense, if the compact set has a complicated shape, the external surface must be also described by a certain distribution of elements). Here, the curvature sign depends on a frame of reference. In the model, the surface normal is assumed to be directed towards the free volume of the pore. Since the normal direction towards the free volume around the compact set is contrary to the direction towards the external-surface curvature center, the curvature sign is negative. Then, changes in the volume of this element V_0 (m^3) will be expressed by the formula:

$$\frac{\partial V_0}{\partial t} = -\sum_j f_{0j}. \quad (9)$$

The initial size distribution of pores elements and the temperature-time mode of sintering are used as the input data in our model that makes it possible to obtain size distribution of pores elements for each time instant in the sintering process. Integral characteristics of the sample i.e. density, surface area with consideration for pores, and linear shrinkage can be calculated from this distribution.

In our model, sintering is considered as redistribution of the surface-elements volume between fractions of these elements and also as the change in the external surface of the sample to be sintered similarly to the change in the internal surface. In other words, vacancies are moving from small pores (large-curvature elements) to large pores (less-curvature elements), and to the external surface (negative-curvature element). Within the model, material properties are described by two constants, i.e. the pre-exponential factor and the activation energy. As the form of equations does not depend on properties of the selected material and also on the powder's initial conditions, then, using appropriate constants, the model must describe sintering kinetics for different materials consisting of chemically stable and chemically non-interacting powders.

At present, it is not quite clear how values of used constants are related to the material properties. Therefore, values of constants are taken so that they could ensure qualitative and quantitative agreement between the calculated and experimental relationships.

2. Ceramics Sintering Experiments

A series of experiments was performed to determine how sintering of alumina ceramics depends on the temperature-time mode. Experiments included preparation and sintering of aluminum-oxide compact sets in different temperature-time modes. The initial powder was a mixture of 80% Al_2O_3 (Pechini)+20% ZrO_2 (3% mol. Y_2O_3).

The laser diffraction method and Malvern Mastersizer 2000 analyzer were used to determine the volumetric distribution of particles in initial powders. Fig. 1 and 2 show dispersiveness measurement results for powders Al_2O_3 и $\text{ZrO}_2(\text{Y}_2\text{O}_3)$. Powder compact sets with the mass of about 0,5 g manufactured with the use of an organic binder were

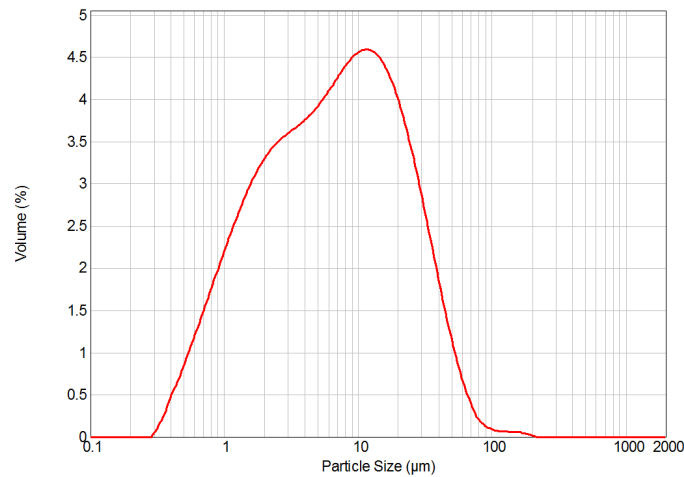


Fig. 1. Volumetric distribution of particles in Al_2O_3 powder

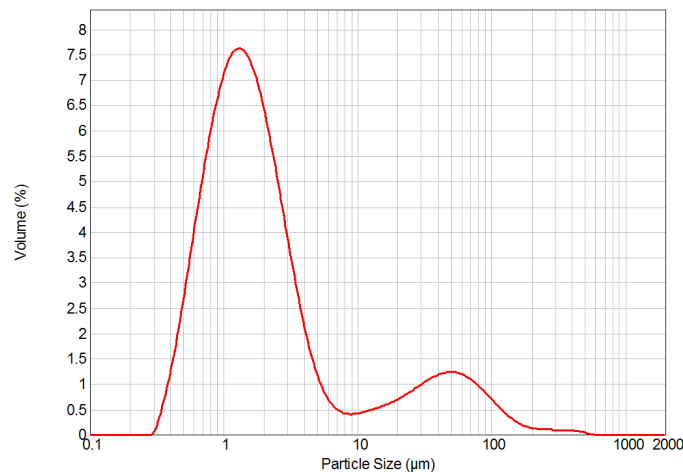


Fig. 2. Volumetric distribution of particles in $\text{ZrO}_2(\text{Y}_2\text{O}_3)$ powder

preliminarily sintered at about 1000°C in order they could acquire transport strength. The binder evaporated in the process of presintering. Then, compact sets obtained in this way were sintered in the air in the following temperature-time modes:

- 1) 25 to 150°C – heating at the rate of $5^\circ\text{C}/\text{min}$ ensures the technological mode when a furnace is warmed up and the high-temperature thermocouple operation begins;
- 2) 150 to 1150°C – heating at the rate of $10^\circ\text{C}/\text{min}$ with the sintering curve recording (linear shrinkage versus time); practically no changes in the samples sizes are observed within this interval;
- 3) 1150 to 1700°C - heating of samples at the rate of 5 , 10 и $15^\circ\text{C}/\text{min}$ min with the curve recording;
- 4) at 1700°C – exposure during 2 hours with the curve recording; main shrinkage of the sample is observed within this interval;
- 5) cooling in the furnace down to the room temperature at the rate of about $30^\circ\text{C}/\text{min}$ without the curve recording.

In the course of sintering, the dilatometer measured the current temperature and the linear shrinkage of samples. Fig. 3 shows "shrinkage versus time" relationships. On the

same time scale, Fig. 4 shows "temperature versus time" relationships for the considered modes.

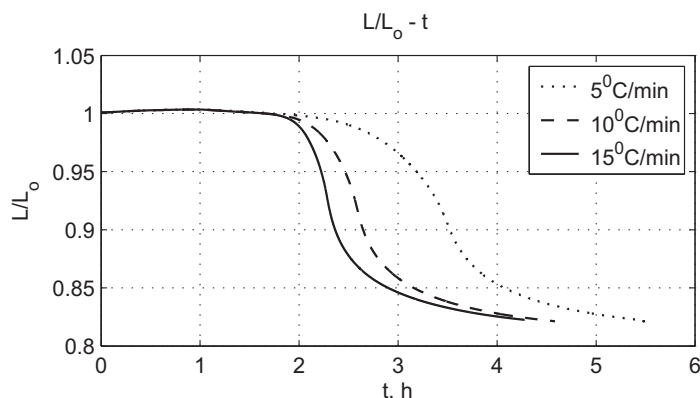


Fig. 3. Shrinkage curves for three temperature-time modes

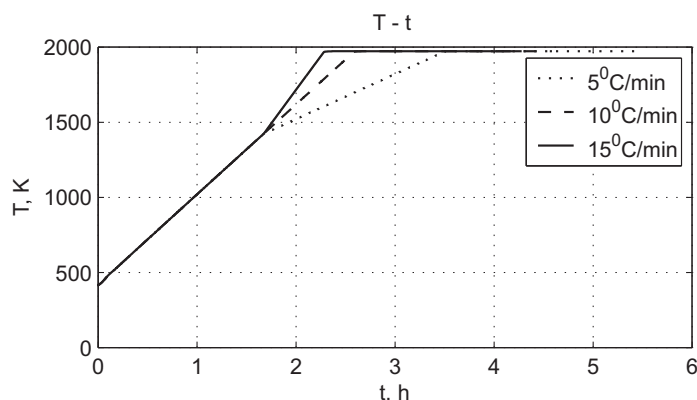


Fig. 4. Temperature-time modes

3. Model Calculations

In order to validate the model and obtain key parameters, we performed series of computations and compared results thereof with the experiment.

Based on the particle-size distribution, it was assumed that radii of pore-forming elements are varying from 0,1 to 100 μm and these elements have the logarithmic-normal size distribution with the maximum at the 10 μm radius. The total number of elements in the considered porous body is taken to be 10^4 . All elements were subdivided into 50 fractions depending on their radii (it is generally thought that each pore can be described as a totality of several elements wherein the number of elements can be less than one). So, the initial distribution took on the form shown in Fig. 5.

Since it is not quite clear how parameters A and E relate to the material properties, several computations were performed with different values of these parameters. The value of activation energy was determined to be responsible for the tangent tilt to the sintering curve in the coordinates "relative linear dimensions of the sample – temperature". The time of high-intensity shrinkage onset depends on the value of the pre-exponential factor. With

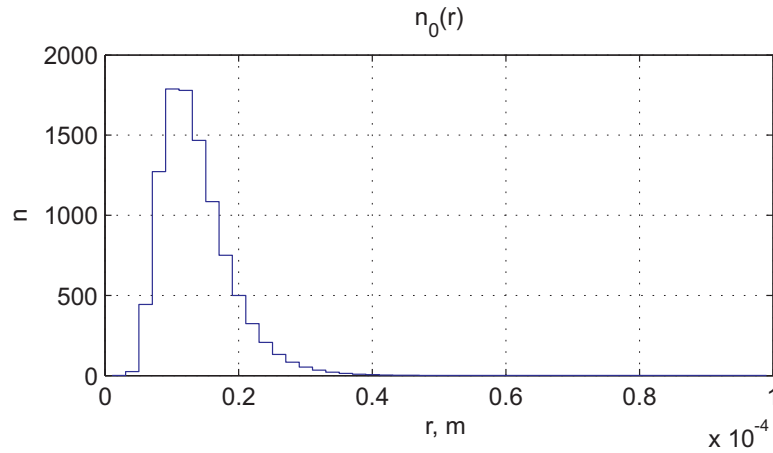


Fig. 5. Initial size distribution of surface elements

consideration for the role of these parameters and on the ground of agreement between the computational and experimental results, we used the activation energy $E = 440$ kJ/mole, and the pre-exponential factor $A = 4,4 \cdot 10^{-31}(\text{m}^{11}/\text{s})$.

In order to understand how the pore volume relates to the total volume of the sample, it is necessary to know the volume ratio of a crystalline material in a porous body. Using the $3,97 \text{ g/cm}^3$ crystalline density of the initial powder (this corresponds to $\alpha - \text{Al}_2\text{O}_3$) [6] and the density of compact sets measured to be $2,18 \text{ g/cm}^3$, the volume fraction of the crystalline material was calculated from the formula:

$$\omega_c = \frac{\rho}{\rho_c}, \quad (10)$$

where ω_c is the volume fraction of the crystalline material, ρ is the measured density of the compact set (g/cm^3), ρ_c is the crystalline density of the material (g/cm^3). The volume fraction of the material was about 54% for all samples.

Using the accepted values of the pre-exponential factor and the activation energy, as well as the initial volume fraction of the crystalline material and the initial distribution of surface elements, the sintering process was calculated for three temperature-time modes realized in the experiment.

Figures 6–8 show experimental (dashed line) and model calculation results (solid lines), as well as the linear thermal expansion calculated for a solid crystal (points). Figures demonstrate that the proposed model enables good qualitative agreement between the calculated shrinkage and the one experimentally observed for the considered temperature-time sintering modes. The maximum difference between the calculated and experimental shrinkage ratings is observed in the experiment with the $5^\circ\text{C}/\text{min}$ heating rate and is equal to 2%.

Conclusion

The paper presents the simplified mathematical model of the sintering process for powders consisting of chemically stable and chemically non-interacting particles (Equations (1), (3) – (9)). The model enables description of the porous material state and

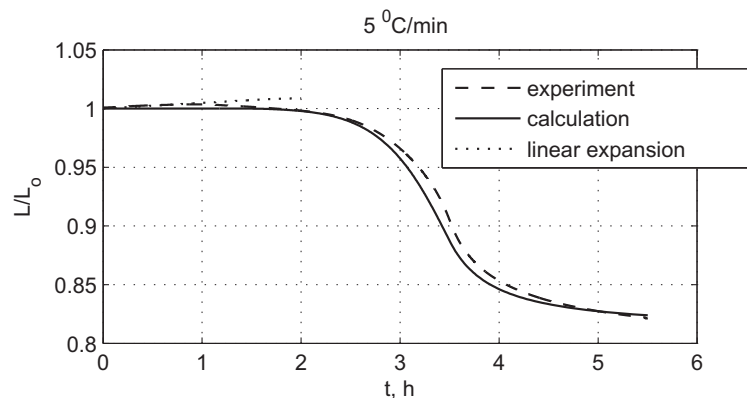


Fig. 6. Calculated and experimental "shrinkage rating versus time" at the 5 °C/min heating rate. Dots show the calculated linear thermal expansion for the solid crystal

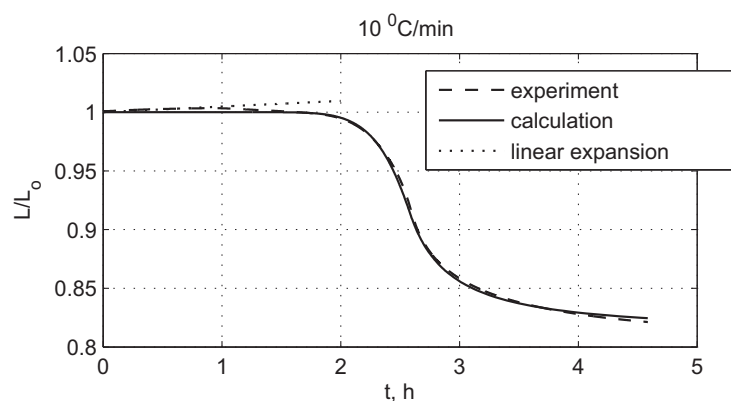


Fig. 7. Calculated and experimental "shrinkage rating versus time" at the 10 °C/min heating rate. Dots show the calculated linear thermal expansion for the solid crystal

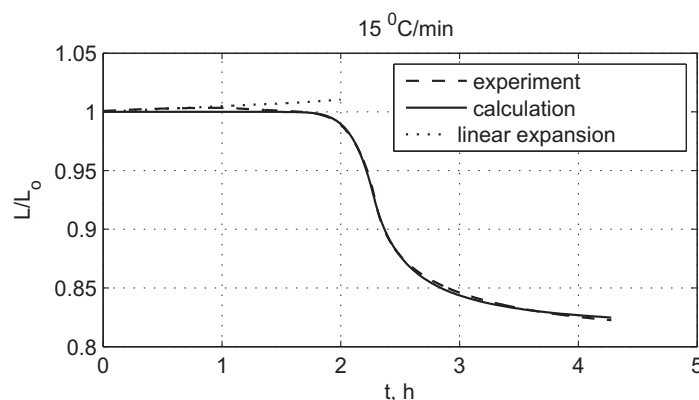


Fig. 8. Calculated and experimental "shrinkage rating versus time" at the 15 °C/min heating rate. Dots show the calculated linear thermal expansion for the solid crystal

time evolution of this material depending on the temperature-time mode of the sintering process.

Alumina ceramics sintering experiments were performed to obtain "shrinkage versus time" relationships for several temperature-time modes.

The experimentally recorded data were used to determine parameters of the model for alumina ceramics. The model is shown to be applicable to alumina ceramics in the range of temperature-time modes realized in the experiment.

For useful comments, authors express their gratitude to V.F. Kuropatenko, Doctor of Science, Professor, Member of St. Petersburg Academy of Sciences.

References

1. Randall M.G. *Sintering Theory and Practice*. N.Y., Wiley, 1996.
2. Rahaman M.N. *Sintering of Ceramics*. Raton, CRC Press, Taylor and Francis Group, 2007.
3. Geguzin Ya.E. *Fizika Spekaniya* [Sintering Physics]. Moscow, Nauka, 1984.
4. Skorokhod V.V. *Reologicheskie Osnovy Teorii Spekaniya* [Reological Basis of Sintering Theory]. Kiev, Naukova Dumka, 1972.
5. Bo Fan. *Numerical Modelling of Sintering of Alumina Pore Shrinkage and Grain Growth*. *Master of Science Thesis*. Delft University of Technology, 2013.
6. Samsonov G.V., Borisova A.L., Zhidkova T.G., Znatokova T.N., Kaloshina Y.P., Kiseleva A.F., Kislyy P.S., Kovalchenko M.S., Kosolapova T.Y., Malakhov Y.S., Malakhov V.Y., Panasyuk A.D., Slavuta V.I., Tkachenko N.I. *Fiziko-khimicheskie svoystva okislov* [Physical-Chemical Properties of Oxides]. Moscow, Metallurgiya, 1978. 472 p.

Received January 12, 2017

УДК 66-93

DOI: 10.14529/mmp170311

МОДЕЛЬ СПЕКАНИЯ ПОРИСТЫХ МАТЕРИАЛОВ

О.В. Шульц, В.А. Симоненко, С.П. Дровосеков, П.В. Капустина, И.А. Белоброва

Российский федеральный ядерный центр – ВНИИ технической физики имени академика Е.И. Забабахина, г. Снежинск

Предложена математическая модель спекания пористых химически стабильных материалов. Исходными данными для модели служат начальное распределение элементов пор по размерам и температурно-временной режим спекания. Спекание моделируется системой кинетических уравнений, описывающих усадку материала в зависимости от его исходного состояния и температурно-временного режима процесса. Были выполнены эксперименты по спеканию алюмооксидного порошка при нескольких температурно-временных режимах, в которых отслеживалась во времени линейная усадка. Предварительно экспериментально было определено начальное распределение частиц исходных порошков по размерам. На основе данных о линейной усадке компактов порошка при скорости нагрева 10 °С/мин были получены значения основных параметров, используемых в модели. Для скоростей нагрева 5 и 15 °С/мин были рассчитаны зависимости линейной усадки от времени. Сравнение рассчитанных зависимостей с экспериментальными данными для скоростей нагрева 5 и 15 °С/мин показало хорошее качественное и количественное согласие.

Ключевые слова: спекание; керамика; математическое моделирование.

Литература

1. Randall, M.G. Sintering Theory and Practice / M.G. Randall. – N.Y.: Wiley, 1996.
2. Rahaman, M.N. Sintering of Ceramics / M.N. Rahaman. – Raton: CRC Press, Taylor and Francis Group, 2007.
3. Гегузин, Я.Е. Физика спекания / Я.Е. Гегузин. – М.: Наука, 1984.
4. Скороход, В.В. Реологические основы теории спекания / В.В. Скороход. – Киев: Наукова Думка, 1972.
5. Bo Fan. Numerical Modelling of Sintering of Alumina Pore Shrinkage and Grain Growth. Master of Science Thesis / Bo Fan. – Delft University of Technology, 2013.
6. Самсонов, Г.В. Физико-химические свойства окислов: справочник / Г.В. Самсонов, А.Л. Борисова, Т.Г. Жидкова и др. – М.: Metallurgia, 1978.

Олег Викторович Шульц, Российский федеральный ядерный центр – ВНИИ технической физики им. академика Е.И. Забабахина (г. Снежинск, Челябинская обл., Российская Федерация), o.v.shults@vniitf.ru.

Вадим Александрович Симоненко, доктор физико-математических наук, профессор, Российский федеральный ядерный центр – ВНИИ технической физики им. академика Е.И. Забабахина (г. Снежинск, Челябинская обл., Российская Федерация), v.a.simonenko@vniitf.ru.

Сергей Петрович Дровосеков, Российский федеральный ядерный центр – ВНИИ технической физики им. академика Е.И. Забабахина (г. Снежинск, Челябинская обл., Российская Федерация), s.p.drovosekov@vniitf.ru.

Полина Вадимовна Капустина, Российский федеральный ядерный центр – ВНИИ технической физики им. академика Е.И. Забабахина (г. Снежинск, Челябинская обл., Российская Федерация), p.v.kapustina@vniitf.ru.

Ирина Андреевна Белоброва, Российский федеральный ядерный центр – ВНИИ технической физики им. академика Е.И. Забабахина (г. Снежинск, Челябинская обл., Российская Федерация), i.a.belobrova@vniitf.ru.

Поступила в редакцию 12 января 2017 г.